

Integrability and conformal bootstrap: One dimensional defect conformal field theory

Andrea Cavaglia^{1,*}, Nikolay Gromov^{1,2,†}, Julius Julius^{1,‡} and Michelangelo Preti^{1,§}

¹Department of Mathematics, King's College London, Strand, London WC2R 2LS, United Kingdom

²St. Petersburg INP, Gatchina, 188 300 St. Petersburg, Russia



(Received 23 August 2021; accepted 3 December 2021; published 7 January 2022)

In this paper we study how the exact nonperturbative integrability methods in 4D $\mathcal{N} = 4$ super-Yang-Mills can work efficiently together with the numerical conformal bootstrap techniques to go beyond the spectral observables and access previously unreachable quantities such as correlation functions at finite coupling. In the setup of 1D defect conformal field theory living on a Maldacena-Wilson line, we managed to compute with good precision a nonsupersymmetric structure constant for a wide range of the 't Hooft coupling. Our result is particularly precise at strong coupling and matches well with the recent analytic results of Meneghelli and Ferrero.

DOI: 10.1103/PhysRevD.105.L021902

I. INTRODUCTION

When it comes to nonperturbative calculations in quantum field theories (QFTs), the number of tools is rather limited. Monte Carlo simulation could give rather accurate results in some theories. In a smaller set of integrable QFTs one can get access to a large number of observables, but usually those theories are limited to 2D. There are a few exceptions, such as $\mathcal{N} = 4$ supersymmetric Yang-Mills (SYM) in 4D, where integrability gives access to nonperturbative physics. The most accurate nonperturbative results are limited to the spectrum of anomalous dimensions, where the quantum spectral curve (QSC) [1,2] method allows one to get extremely precise results at 't Hooft coupling $\lambda \simeq 1$ (for example 60 digits in [3] for the Balitsky-Fadin-Kuraev-Lipatov Pomeron intercept).

In this paper we focus on planar $\mathcal{N} = 4$ SYM. As a conformal theory, for its complete solution, in addition to the dimensions of the operators, one also needs to know the operator product expansion (OPE) coefficients or structure constants. Even though there have been many exciting applications of integrability to the study of the structure constants [4–7], these results are either limited to perturbation theory, infinitely long operators, strongly γ -deformed

(Fishnet) theories, or are not explicit enough for numerical evaluation.

Another powerful nonperturbative method to study conformal field theories (CFTs) is the numerical conformal bootstrap (NCB) (see [8–10] for some reviews). It allows one to identify prohibited domains for the conformal dimensions or OPE coefficients given the symmetries of the CFT as an input. However, it may happen that an interesting physical theory lies deep within the bounds given by the conformal bootstrap, rather than on the

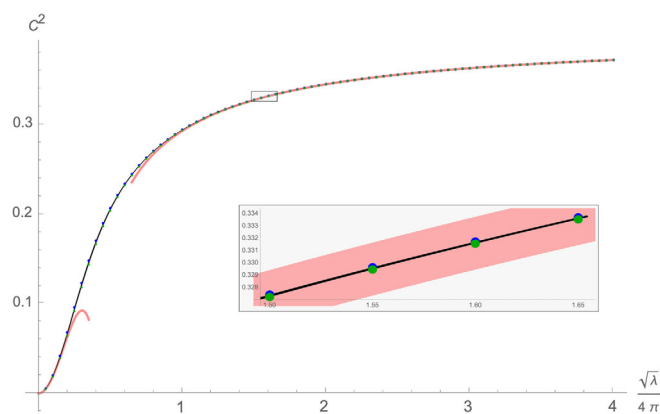


FIG. 1. The OPE coefficient of two protected line-deformation operators Φ_{\perp}^i into unprotected operator Φ_{\parallel} . The thickness of the black line indicates the precision. The interval of values of $g = \frac{\sqrt{\lambda}}{4\pi}$ spans a wide range in $\lambda \in (0, 2526.6)$. It interpolates perfectly between the weak [18,19] and strong [11,20,21] coupling analytic results indicated by thick pink lines. We see that already at $g = 1.5$ our result matches perfectly the three-loop result of [21], obtained by a very different method. At weak coupling we compare with the preliminary result $2g^2 + \frac{4}{3}(\pi^2 - 18)g^4$ of [19].

* andrea.cavaglia@kcl.ac.uk

† nikolay.gromov@kcl.ac.uk

‡ julius.julius@kcl.ac.uk

§ michelangelo.preti@kcl.ac.uk

Published by the American Physical Society under the terms of the Creative Commons Attribution 4.0 International license. Further distribution of this work must maintain attribution to the author(s) and the published article's title, journal citation, and DOI. Funded by SCOAP³.

boundary. In this scenario, which seems to apply to the interesting case of conformal gauge theories at finite values of the coupling (see e.g. the cases studied in [11,12]), one can only extract a limited amount of information from the bootstrap constraints in the nonperturbative regime.

In this paper, we initiate a strategy to overcome these limitations by combining the two powerful methods of QSC and NCB. Specifically, we consider nonlocal operators realized as insertions on an infinite supersymmetric Wilson line in the 4D theory. Their correlators are constrained by a 1D version of the conformal bootstrap. We will show how, using exact spectral data coming from the QSC as an input for the NCB, accurate values for a nontrivial structure constant of such nonlocal operators can be obtained in a wide range of the coupling (see Fig. 1). This result would not be reachable by any present method based purely on integrability or the conformal bootstrap. While the strategy of supplementing conformal bootstrap equations with extra spectral data has been applied in other contexts [13–17], this is the first time its effectiveness is demonstrated for observables in a higher-dimensional gauge theory.

We remark that there is also hope for an integrability based nonperturbative analytical solution for correlators in planar $\mathcal{N} = 4$ SYM, for example built upon the separation of variables approach [5,22]. The strategy we introduce with this paper provides an alternative method to generate high precision data for future comparison. We also expect that the synergy with bootstrap methods will be able to consistently push the frontier of what can be achieved by integrability alone.

II. SETUP

Here we focus on the one dimensional defect CFT that lives on the infinite straight 1/2-Bogomol’nyi-Prasad-Sommerfield (BPS) Maldacena-Wilson line (MWL) in $\mathcal{N} = 4$ SYM defined by [23,24]

$$\mathcal{W} = \text{Tr}W_{-\infty}^{+\infty} \equiv \text{TrP} \exp \int_{-\infty}^{+\infty} dt(iA_t + \Phi_{\parallel}). \quad (1)$$

Φ_{\parallel} is one of the six real scalars. We denote the remaining five scalars by Φ_{\perp}^i . The MWL preserves an $\text{OSp}(4^*|4)$ subgroup of the symmetry of $\mathcal{N} = 4$ SYM. It includes an $\text{SO}(5)_R$ subgroup of R symmetry, the 1D conformal group $\text{SO}(1,2)$ and the $\text{SO}(3)$ group of rotations in the subspace orthogonal to the line [25]. We mention that a similar line defect CFT setup was also considered in the 3D Aharony-Bergman-Jafferis-Maldacena theory, see [26,27], and the related conformal bootstrap was studied in [28], while the integrability side is not fully developed yet [29].

Correlation functions in the defect CFT are the expectation values of the Wilson line with insertions of local operators [20,22,32–37]:

$$\begin{aligned} & \langle\langle \mathcal{O}_1(t_1) \mathcal{O}_2(t_2) \cdots \mathcal{O}_n(t_n) \rangle\rangle \\ & \equiv \langle \text{Tr} W_{-\infty}^{t_1} \mathcal{O}_1(t_1) W_{t_1}^{t_2} \mathcal{O}_2(t_2) \cdots \mathcal{O}_n(t_n) W_{t_n}^{+\infty} \rangle, \end{aligned} \quad (2)$$

where $W_{t_i}^{t_j}$ is a segment of the line (1).

An important role is played by so-called line-deformation BPS multiplets \mathcal{B}_n . For example the simplest \mathcal{B}_1 super-multiplet contains Φ_{\perp}^i as its top component. As a consequence, the dimension of this operator is protected and equal to 1. The simplest nonprotected operator is Φ_{\parallel} [11,25,36,38].

In addition to conformal symmetry, $\mathcal{N} = 4$ SYM also exhibits integrability, which controls the spectrum of the defect CFT as we describe in the next section.

III. QSC AND THE SPECTRUM

The two point functions of conformal primary operators are controlled by the conformal dimensions $\langle\langle \mathcal{O}_A(t_1) \mathcal{O}_B(t_2) \rangle\rangle \propto \delta_{AB} |t_1 - t_2|^{-2\Delta_A}$. Initially, thermodynamic Bethe ansatz equations describing the spectrum of some operators were written in [33,39], which then were transformed into a QSC form more suitable for practical calculations in [40], but for a long time it was not clear if integrability could also compute dimensions of “neutral” operators such as Φ_{\parallel} . In [38] it was shown that the straight-line limit of the QSC of [40] captures those operators too. It is currently expected that all operators appearing in this defect CFT can be studied in a similar way. In particular we computed solutions of the QSC for all operators with nontrivial anomalous dimensions appearing in the OPE of $\Phi_{\perp}^i \times \Phi_{\perp}^j$ with bare dimensions $\Delta_0 = 1, 2, 3$, and further solutions for $\Delta_0 = 4, 5$ and 6 for a total of 35 states (see Fig. 2).

A. QSC

For the details of the QSC constructions we refer to recent reviews [42–44]. Let us briefly summarize the construction: there are $4 + 4$ functions \mathbf{p}_a and \mathbf{q}_i of one complex variable u , which are related by some finite difference relations. All these functions have a quadratic branch cut starting at $\pm 2g$ in the complex plane of u . Introducing $x(u) = \frac{u + \sqrt{u - 2g} \sqrt{u + 2g}}{2g}$ one can represent \mathbf{p}_a functions as an expansion $\mathbf{p}_a = \sum_n \frac{c_{a,n}}{x^n}$. After that one solves for \mathbf{q}_i , which satisfy a finite difference equation in u with coefficients built out of \mathbf{p} ’s. To select physical states, one has to impose the “gluing condition” $\mathbf{q}_k(u \pm i0) = M_k^j \mathbf{q}_j(-u \pm i0)$ for $u \in [-2g, 2g]$, where $M_1^1 = 1$, $M_2^2 = -M_4^4 = \alpha \sinh(2\pi u)$ and other elements 0, which fixes the coefficients $c_{a,n}$ to a discrete set of values. The dimensions Δ can be read off the large u asymptotics: $\mathbf{q}_i(u) \sim u^{n_i + \Delta}$ (for some integers n_i).

In order to find this large number of states, we have to resolve the main technical problem preventing us from getting good starting points for the numerical algorithm. We reformulate the optimization problem for finding the coefficients in \mathbf{p}_a into the search for the zeros of a vector function for Fourier modes of the gluing condition, which we then solve with the Newton method. Details of the construction will be published elsewhere [19]. This method is significantly more stable at weak coupling and allows us to use the perturbative analytical solutions of the QSC (for example [3,45,46]) as starting points for the numerical algorithm efficiently even for highly excited states.

B. States

The nonprotected states appearing in the OPE of two \mathcal{B}_1 multiplets should have all quantum numbers zero (except Δ) [11]. In general the mixing problem is quite complicated and there are no simple closed sectors. However, at one loop, mixing is limited. For example the scalars Φ_{\parallel} and $\Phi_{\perp}^i \Phi_{\perp}^i$ form a closed sector and the mixing matrix is known explicitly [47]. We notice that the spectrum of this mixing matrix coincides exactly with the spectrum of a one-loop PSU(2,2|4) effective Bethe ansatz for a particular choice of Bethe roots numbers. It is convenient to use the oscillator notation [48–51], which translates into roots numbers easily (see e.g. [52]). For those states we find $n_{\mathbf{f}_i} = \{\Delta_0 + 1, \Delta_0 + 1, \Delta_0, \Delta_0\}$ and $n_{\mathbf{a}_i} = n_{\mathbf{b}_i} = 0$. Plugging those numbers into the Bethe ansatz equation solver of [52], and selecting states satisfying a parity in u (accompanied with a flip of the Dynkin diagram), we reproduce the spectrum of the mixing matrix of [47]. Having this one-loop solution, we use it as a starting point for the iterative procedure [3] to obtain a four-loop analytico-numerical solution of the QSC (keeping 200 digits precision). This is then fed into the purely numerical

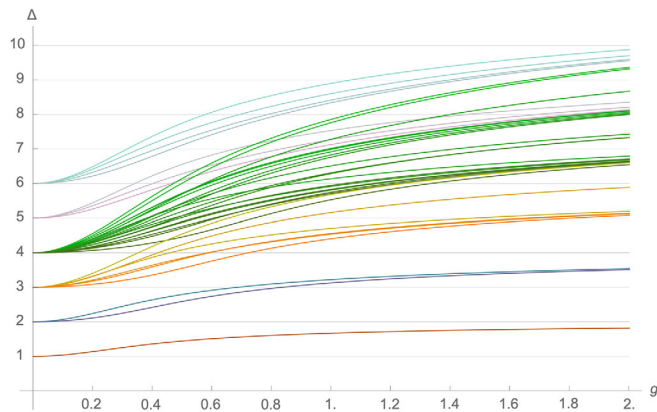


FIG. 2. Dimensions of 35 states computed with high precision with the QSC using an improved method of [19]. For several lowest lying states we have data in a wider range $g \in [0, 4]$. The oscillator content and one-loop anomalous dimensions of the states are given in Table I of the Supplemental Material [41].

algorithm of [53] with the new implementation of the optimization problem. In this way we obtain high precision (around 20 digits) data for the spectrum (see Fig. 2). The fact that those initial points lead to a convergent procedure for the QSC at finite g is a very nontrivial test of the above construction.

In addition to the scalar sector, other states can, for example, include covariant derivatives \mathcal{D}_t and also some combinations of fermions.

The simplest way to describe those states at one loop is again by means of the effective “doubling-trick” oscillator numbers $[n_{\mathbf{a}_1}, n_{\mathbf{a}_2} | n_{\mathbf{f}_1}, n_{\mathbf{f}_2}, n_{\mathbf{f}_3}, n_{\mathbf{f}_4} | n_{\mathbf{b}_1}, n_{\mathbf{b}_2}]$, which in general have to be set to

$$[\Delta_0 - T, \Delta_0 - T | 1 + T, 1 + T, T, T | \Delta_0 - T, \Delta_0 - T], \quad (3)$$

where $\Delta_0 - T$, roughly, corresponds to the number of covariant derivatives \mathcal{D}_t (which can also potentially mix with fermions even at one loop). Note that, whereas T changes the Bethe roots numbers, it does not affect the quantum numbers of the states. One can call the parameter T a twist, in analogy with higher dimensional cases. Above, $T = 2, \dots, \Delta_0$, except for $\Delta_0 = 1$ where $T = 1$ (this state is exceptional as it satisfies a semishortening condition at weak coupling). The oscillator numbers (3) then lead to a set of one-loop states, which are used for numerical calculation as before.

At weak coupling, for $\Delta_0 = 1, 2, 3$ our procedure produces 1,2,6 solutions respectively, in agreement with the counting produced by free field theory. For $\Delta_0 = 4$, we computed 19 levels. These are all states with a parity symmetry of the solutions of the QSC, and are possibly not an exhaustive list. We postpone clarifying this point to future work, as our bootstrap results do not rely on these states. From $\Delta_0 = 5$ onward, we only solved for twist-2 states, which dominate at weak coupling, as they are the only ones with order $O(1)$ OPE coefficients (this can be seen at tree level in perturbation theory).

All of the states we found proceed to constant integers Δ_{∞} at strong coupling, in contrast with the early expectations [54] and also very different to the spectrum of local operators, where all unprotected states scale to infinity. For $\Delta_{\infty} = 2, 4, 6, 7, 8$, we found 1,2,4,1,9 states respectively, which matches with the counting of [55]. As we only computed 35 states, at higher Δ_{∞} , we already miss some levels (for example for $\Delta_{\infty} = 9$ we are two states short).

IV. FOUR-POINT FUNCTION AND CROSSING SYMMETRY

In order to extract the structure constant C_1 we consider the correlator of four arbitrary operators belonging to the contour deformation multiplet \mathcal{B}_1 . All such four-point functions are related and can be expressed in terms of a single nontrivial function $f(\chi)$ [11,21,25] thanks to the

analytic superspace formalism of [56]. For example for four identical scalars,

$$\begin{aligned} & \langle\langle \Phi_{\perp}^1(x_1)\Phi_{\perp}^1(x_2)\Phi_{\perp}^1(x_3)\Phi_{\perp}^1(x_4) \rangle\rangle \\ &= \frac{F\chi^2 + (2\chi^{-1} - 1)f - (\chi^2 - \chi + 1)f'}{x_{12}^2 x_{34}^2}, \end{aligned} \quad (4)$$

where $\chi = \frac{x_{12}x_{34}}{x_{13}x_{24}}$, $x_{ij} = x_i - x_j$. Finally, $F = 1 + C_{\text{BPS}}^2 = \frac{3WW''}{(W')^2}$ with $W = \frac{2I_1(\sqrt{\lambda})}{\sqrt{\lambda}}$ [24,57,58]. The function (4) has a symmetry under the cyclic permutation of the coordinates x_i , which translates into the crossing equation:

$$(1 - \chi)^2 f(\chi) + \chi^2 f(1 - \chi) = 0. \quad (5)$$

Furthermore, since Φ_{\perp}^1 is a superconformal primary $f(\chi)$ can be decomposed into a sum over conformal blocks

$$f(\chi) = \chi + C_{\text{BPS}}^2 F_{B_2}(\chi) + \sum_n C_n^2 F_{\Delta_n}(\chi), \quad (6)$$

where $F_{B_2} = \chi - \chi_2 F_1(1, 2, 4; \chi)$ and

$$F_{\Delta} = \frac{\chi^{\Delta+1}}{1 - \Delta} {}_2F_1(\Delta + 1, \Delta + 2, 2\Delta + 4; \chi). \quad (7)$$

It is clear that the equation (5) can be written as

$$\sum_n C_n^2 G_{\Delta_n}(\chi) = H(\chi), \quad (8)$$

where the functions G and H are known. Assuming that we have access to the full spectrum, (8) becomes a system of linear equations for C_n^2 . An obvious problem is that (8) contains an infinite number of equations (by picking various values of χ) for an infinite number of unknowns $\{C_n^2\}_{n=1}^{\infty}$. As we managed to compute a large number of low lying states Δ_n from integrability, the main hurdle is finding an efficient truncation scheme which would allow one to obtain a good approximation (at least numerically) for the OPE coefficients C_n^2 . In the next section we describe several possibilities and our main result for C_1^2 given in Fig. 1.

V. SOLVING THE CROSSING EQUATION

In this section we report on various attempts to truncate the crossing equation (7) to a finite dimensional system.

A. Pointlike functionals

One of the obvious ways to get a finite system out of (7) is to truncate the sum at some level Δ_N and sample N different values of the cross-ratio χ_i . One can then solve a $N \times N$ linear system for the OPE coefficients $a_n \equiv C_n^2$. Assuming the procedure converges, different sets of points

$\{\chi_i\}$ should give similar results, but in practice that is not the case. It was proposed in [16] to average the result over a large number of sampling sets, and use the statistical variance of a_n as an error estimate. Even though this method at the first sight is quite unusual, it does give good results in situations where the density of the spectrum does not increase too fast with Δ . Indeed it worked well in the context of the 2D critical lattice models studied in [16,17].

In our case, the number of states increases rapidly and this method gives almost 100% error in the intermediate coupling region. Similar problems were observed also by the authors of [17].

We attempted to improve the method slightly by making it more deterministic. First we rewrite the truncated equation (8) as $\sum_{n=0}^N a_n G_n(\chi) = 0$ with $G_0 = H$ and $a_0 = -1$. Then we sample $M > N$ points χ_i and find a_n by minimization of

$$S(\{a_n\}) = \sum_{i=1}^M \left[\sum_{n=0}^N a_n G_n(\chi_i) \right]^2. \quad (9)$$

This method converges better, but still gives large error bars in our case. Again, for a spectrum whose density does not grow too fast it works well, e.g. for the free spectrum $\Delta_n = 2n$ it gives for $N = 6$ the known result $a_1 = \frac{2}{5}$ with 7 digits. This number also gives the strong coupling asymptote of our result in Fig. 1.

B. Oscillating optimized functionals

In a more abstract way, one can define a linear functional α which, when acting on $G_{\Delta_n}(\chi)$, returns a number $\omega(\Delta_n)$. For the case of the pointlike functional, α simply evaluates its argument as some point χ_i . In order for the procedure of extracting the OPE coefficients to work well, one should make sure that $\omega(\Delta)$ is decaying fast at large Δ . Whereas the pointlike functional does decay with Δ , one can construct much faster decaying functionals. A simple way is to look for such functionals in the form

$$\alpha[f] = \sum_{n=0}^{N/2} c_n \partial^{2n} f(\chi)|_{\chi=1/2} \quad (10)$$

for some large N . One can find the coefficients c_n from the requirement that the corresponding $\omega(\Delta)$ is small (with respect to a suitable measure) for all $\Delta > \Delta_g$. This type of functionals allows one to truncate the system very efficiently and give a result for C_1^2 , consistent with more traditional optimal positive functionals, which we describe below. The advantage of this method is that it does not require positivity of the OPE coefficients C_n^2 and thus could be used for nonunitary theories. The disadvantage is that estimating the error of the approximation requires extra effort, whereas the positive functionals give exclusion

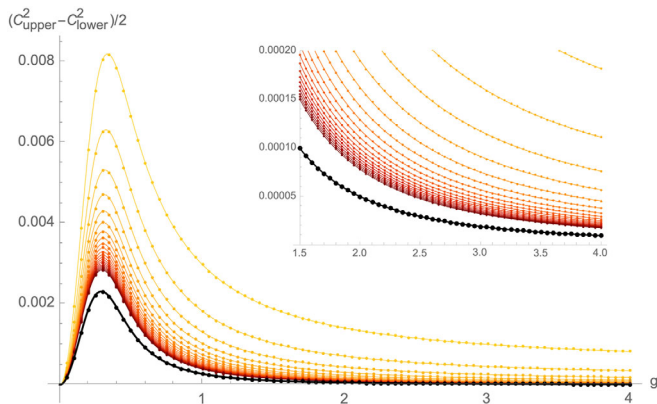


FIG. 3. The orange lines show half of the difference between upper and lower bound for $N = 5, 7, \dots, 45$ number of nontrivial derivatives. The black line is an extrapolation to an infinite number of derivatives. Thus, it gives our estimate for the upper limit of the error of our result.

domains from which one can estimate the error immediately.

C. Optimal positive functionals

A more standard NCB approach is to use optimized functionals which are positive above $\Delta > \Delta_g$. The SDPB package [59,60] allows one to find such functionals easily. For example, SDPB can find c_n from (10) such that $\omega(\Delta) > 0$ for $\Delta > \Delta_g$, $\omega(\Delta_1) = \pm 1$ and $\alpha[H]$ is minimal. It is easy to see that then $\pm\alpha[H]$ gives the upper/lower bound for C_1^2 if there are no states in the interval (Δ_1, Δ_g) . This method works very well in our case, by taking $\Delta_g = \Delta_2$ we get a very narrow allowed interval for C_1^2 (Fig. 1). Half of the length of this interval gives the error of our result as shown on Fig. 3. The precision of this method increases with the number of terms in the sum (10). By computing the bounds for $N = 5, 7, \dots, 45$ we found that a $1/N$ fit gives a very stable prediction for the $N = \infty$ limit, with $\sim 10^{-7}$ extrapolation error, which is also shown in Fig. 3 by a thick black line. This gives our final estimate for the error of our result for C_1^2 . We see that the estimation for C_1^2 works the best above $g > 1$, but even at smaller coupling the absolute error is $\lesssim 0.0023$, it decreases quickly to $\lesssim 0.0001$ for $g = 1.5$ and for $g = 4$ it reaches $\lesssim 0.00001$. The full result is given in the Supplemental Material [41].

D. Incorporating higher states

What is very striking is that the NCB already gives very precise bounds given only two states Δ_1 and Δ_2 as an input. In order to improve it further one can consider more states and different types of optimization problems. The numerical analysis with current methods becomes more complicated. Here we present some preliminary results, which incorporate two more states.

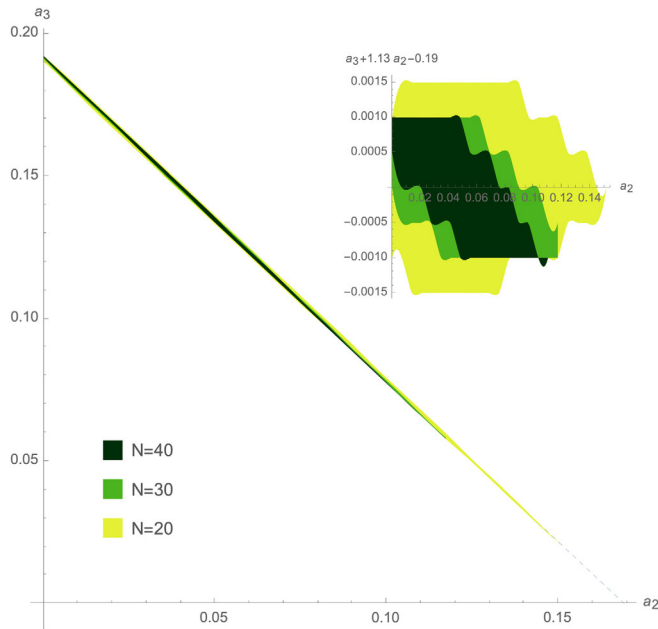


FIG. 4. Bounds for OPE coefficients $a_2 = C_2^2$, $a_3 = C_3^2$ of the two higher states of bare dimension 2 for $g = 1$. The very narrow allowed domain is situated along the line $a_3 + 1.13a_2 = 0.19$ (dashed line), which shrinks further with increased N .

In Fig. 4 we plot the allowed regions for C_2 and C_3 . The NCB gives a very narrow domain, which shrinks further with increased N . The reason the domain is stretched in one direction is the fact that these two states are situated rather close to each other, and it requires higher resolution and large N to resolve between them. Notably, for each allowed value of C_2 and C_3 the corresponding allowed region for C_1 is much narrower than we found previously. This gives hope that the bounds on C_1 could be further improved. It remains, however, an open question if one can reach an arbitrary high precision for C_1 , or if there is a fundamental limit. We reserve these questions for future study.

VI. CONCLUSIONS

The combination of integrability and conformal bootstrap methods gave us surprisingly precise results. Yet we only used a small amount of data available from integrability. In addition to obvious things such as incorporating more states and increasing numerical precision, we believe there is more information from the integrability side which can be incorporated in the current setup [19]. Moreover, more constraints come from considering the OPE decomposition of more correlators. We expect that using these approaches it will be possible to improve the bounds on the OPE coefficients, and obtain accurate predictions also for excited states.

Another direction would be to try to use the combination of QSC and NCB in order to extract bulk CFT data.

Crossing equations in 4D can provide more constraints than the 1D crossing we use here.

The type of problem we considered here may require some further development on the NCB side. For example, when the spectrum is partially known, one can relax the positivity requirement in the intervals between the states, which would potentially give tighter bounds on the OPE coefficients.

In conclusion, whereas we cannot yet claim with certainty that

QSC + conformal bootstrap = solution of SYM

we have produced clear evidence that these two methods work well together, giving us rich insights about the nonperturbative regime of planar $\mathcal{N} = 4$ SYM.

ACKNOWLEDGMENTS

We thank P. Ferrero, Y. He, A. Stergiou, D. Volin and especially C. Meneghelli for insightful discussions. J. J. is grateful to M. Trépanier for helpful discussions. J. J. acknowledges the computing resources at Morphing Machines and the CAD Lab at the Indian Institute of Science which were used to obtain some of the numerical results, and thanks H. Chambeti, S. K. Nandy and R. Narayan for the same. M. P. thanks A. Manenti for useful discussions. The work of A. C., N. G. and M. P. is supported by European Research Council (ERC) under the European Union's Horizon 2020 research and innovation program (Grant Agreement No. 865075) EXACTC. N. G. is also partially supported by the STFC Grant No. ST/P000258/1.

-
- [1] N. Gromov, V. Kazakov, S. Leurent, and D. Volin, Quantum Spectral Curve for Planar $\mathcal{N} = 4$ Super-Yang-Mills Theory, *Phys. Rev. Lett.* **112**, 011602 (2014).
 - [2] N. Gromov, V. Kazakov, S. Leurent, and D. Volin, Quantum spectral curve for arbitrary state/operator in $\text{AdS}_5/\text{CFT}_4$, *J. High Energy Phys.* 09 (2015) 187.
 - [3] N. Gromov, F. Levkovich-Maslyuk, and G. Sizov, Pomeron Eigenvalue at Three Loops in $N = 4$ Supersymmetric Yang-Mills Theory, *Phys. Rev. Lett.* **115**, 251601 (2015).
 - [4] B. Basso, S. Komatsu, and P. Vieira, Structure constants and integrable bootstrap in planar $N = 4$ SYM theory, [arXiv:1505.06745](https://arxiv.org/abs/1505.06745).
 - [5] A. Cavaglià, N. Gromov, and F. Levkovich-Maslyuk, Quantum spectral curve and structure constants in $\mathcal{N} = 4$ SYM: Cusps in the ladder limit, *J. High Energy Phys.* 10 (2018) 060.
 - [6] Y. Jiang, S. Komatsu, and E. Vescovi, Exact Three-Point Functions of Determinant Operators in Planar $N = 4$ Supersymmetric Yang-Mills Theory, *Phys. Rev. Lett.* **123**, 191601 (2019).
 - [7] A. Cavaglià, N. Gromov, and F. Levkovich-Maslyuk, Separation of variables in AdS/CFT : Functional approach for the fishnet CFT, *J. High Energy Phys.* 06 (2021) 131.
 - [8] D. Simmons-Duffin, The conformal bootstrap, in *Theoretical Advanced Study Institute in Elementary Particle Physics: New Frontiers in Fields and Strings* (World Scientific, Singapore, 2016).
 - [9] D. Poland, S. Rychkov, and A. Vichi, The conformal bootstrap: Theory, numerical techniques, and applications, *Rev. Mod. Phys.* **91**, 015002 (2019).
 - [10] S. M. Chester, Weizmann lectures on the numerical conformal bootstrap, [arXiv:1907.05147](https://arxiv.org/abs/1907.05147).
 - [11] P. Liendo, C. Meneghelli, and V. Mitev, Bootstrapping the half-BPS line defect, *J. High Energy Phys.* 10 (2018) 077.
 - [12] C. Beem, L. Rastelli, and B. C. van Rees, More $\mathcal{N} = 4$ superconformal bootstrap, *Phys. Rev. D* **96**, 046014 (2017).
 - [13] F. Gliozzi, P. Liendo, M. Meineri, and A. Rago, Boundary and interface CFTs from the conformal bootstrap, *J. High Energy Phys.* 05 (2015) 036.
 - [14] F. Gliozzi, Truncatable bootstrap equations in algebraic form and critical surface exponents, *J. High Energy Phys.* 10 (2016) 037.
 - [15] Y. Nakayama, Bootstrapping Critical Ising Model on Three-Dimensional Real Projective Space, *Phys. Rev. Lett.* **116**, 141602 (2016).
 - [16] M. Picco, S. Ribault, and R. Santachiara, A conformal bootstrap approach to critical percolation in two dimensions, *SciPost Phys.* **1**, 009 (2016).
 - [17] Y. He, J. L. Jacobsen, and H. Saleur, Geometrical four-point functions in the two-dimensional critical Q -state Potts model: The interchiral conformal bootstrap, *J. High Energy Phys.* 12 (2020) 019.
 - [18] N. Kiryu and S. Komatsu, Correlation functions on the Half-BPS Wilson loop: Perturbation and hexagonalization, *J. High Energy Phys.* 02 (2019) 090.
 - [19] A. Cavaglià, N. Gromov, J. Julius, and M. Preti (to be published).
 - [20] S. Giombi, R. Roiban, and A. A. Tseytlin, Half-BPS Wilson loop and $\text{AdS}_2/\text{CFT}_1$, *Nucl. Phys.* **B922**, 499 (2017).
 - [21] P. Ferrero and C. Meneghelli, Bootstrapping the half-BPS line defect CFT in $\mathcal{N} = 4$ SYM at strong coupling, *Phys. Rev. D* **104**, L081703 (2021).
 - [22] S. Giombi and S. Komatsu, Exact correlators on the Wilson loop in $\mathcal{N} = 4$ SYM: Localization, defect CFT, and integrability, *J. High Energy Phys.* 05 (2018) 109; 11 (2018) 123(E).
 - [23] J. M. Maldacena, Wilson Loops in Large N Field Theories, *Phys. Rev. Lett.* **80**, 4859 (1998).
 - [24] J. K. Erickson, G. W. Semenoff, and K. Zarembo, Wilson loops in $N = 4$ supersymmetric Yang-Mills theory, *Nucl. Phys.* **B582**, 155 (2000).

- [25] P. Liendo and C. Meneghelli, Bootstrap equations for $\mathcal{N} = 4$ SYM with defects, *J. High Energy Phys.* **01** (2017) 122.
- [26] L. Bianchi, L. Griguolo, M. Preti, and D. Seminara, Wilson lines as superconformal defects in ABJM theory: A formula for the emitted radiation, *J. High Energy Phys.* **10** (2017) 050.
- [27] L. Bianchi, M. Preti, and E. Vescovi, Exact Bremsstrahlung functions in ABJM theory, *J. High Energy Phys.* **07** (2018) 060.
- [28] L. Bianchi, G. Bliard, V. Forini, L. Griguolo, and D. Seminara, Analytic bootstrap and Witten diagrams for the ABJM Wilson line as defect CFT₁, *J. High Energy Phys.* **08** (2020) 143.
- [29] The QSC is known for the spectrum of local operators in ABJM theory [30,31], but its version for the defect CFT is still unknown.
- [30] A. Cavaglià, D. Fioravanti, N. Gromov, and R. Tateo, Quantum Spectral Curve of the $N = 6$ Supersymmetric Chern-Simons Theory, *Phys. Rev. Lett.* **113**, 021601 (2014).
- [31] D. Bombardelli, A. Cavaglià, D. Fioravanti, N. Gromov, and R. Tateo, The full quantum spectral curve for AdS₄/CFT₃, *J. High Energy Phys.* **09** (2017) 140.
- [32] N. Drukker and S. Kawamoto, Small deformations of supersymmetric Wilson loops and open spin-chains, *J. High Energy Phys.* **07** (2006) 024.
- [33] N. Drukker, Integrable Wilson loops, *J. High Energy Phys.* **10** (2013) 135.
- [34] D. Correa, J. Henn, J. Maldacena, and A. Sever, An exact formula for the radiation of a moving quark in $N = 4$ super Yang Mills, *J. High Energy Phys.* **06** (2012) 048.
- [35] M. Bonini, L. Griguolo, M. Preti, and D. Seminara, Bremsstrahlung function, leading Lüscher correction at weak coupling and localization, *J. High Energy Phys.* **02** (2016) 172.
- [36] M. Cooke, A. Dekel, and N. Drukker, The Wilson loop CFT: Insertion dimensions and structure constants from wavy lines, *J. Phys. A* **50**, 335401 (2017).
- [37] S. Giombi and S. Komatsu, More exact results in the Wilson loop defect CFT: Bulk-defect OPE, nonplanar corrections and quantum spectral curve, *J. Phys. A* **52**, 125401 (2019).
- [38] D. Grabner, N. Gromov, and J. Julius, Excited states of one-dimensional defect CFTs from the quantum spectral curve, *J. High Energy Phys.* **07** (2020) 042.
- [39] D. Correa, J. Maldacena, and A. Sever, The quark anti-quark potential and the cusp anomalous dimension from a TBA equation, *J. High Energy Phys.* **08** (2012) 134,
- [40] N. Gromov and F. Levkovich-Maslyuk, Quantum spectral curve for a cusped Wilson line in $\mathcal{N} = 4$ SYM, *J. High Energy Phys.* **04** (2016) 134.
- [41] See Supplemental Material at <http://link.aps.org/supplemental/10.1103/PhysRevD.105.L021902> for explicit numerical data to support the claims of the paper.
- [42] N. Gromov, Introduction to the spectrum of $N = 4$ SYM and the quantum spectral curve, [arXiv:1708.03648](https://arxiv.org/abs/1708.03648).
- [43] V. Kazakov, Quantum spectral curve of γ -twisted $\mathcal{N} = 4$ SYM theory and fishnet CFT, *Rev. Math. Phys.* **30**, 1840010 (2018).
- [44] F. Levkovich-Maslyuk, A review of the AdS/CFT quantum spectral curve, *J. Phys. A* **53**, 283004 (2020).
- [45] C. Marboe and D. Volin, Quantum spectral curve as a tool for a perturbative quantum field theory, *Nucl. Phys.* **B899**, 810 (2015).
- [46] C. Marboe and D. Volin, The full spectrum of AdS₅/CFT₄ II: Weak coupling expansion via the quantum spectral curve, *J. Phys. A* **54**, 055201 (2021).
- [47] D. Correa, M. Leoni, and S. Luque, Spin chain integrability in nonsupersymmetric Wilson loops, *J. High Energy Phys.* **12** (2018) 050.
- [48] I. Bars and M. Gunaydin, Unitary representations of noncompact supergroups, *Commun. Math. Phys.* **91**, 31 (1983).
- [49] M. Gunaydin and N. Marcus, The spectrum of the S⁵ compactification of the chiral $N = 2$, $D = 10$ supergravity and the unitary supermultiplets of $U(2,2/4)$, *Classical Quantum Gravity* **2**, L11 (1985).
- [50] N. Beisert, The complete one loop dilatation operator of $N = 4$ super-Yang-Mills theory, *Nucl. Phys.* **B676**, 3 (2004).
- [51] N. Beisert, The dilatation operator of $N = 4$ super Yang-Mills theory and integrability, *Phys. Rep.* **405**, 1 (2004).
- [52] C. Marboe and D. Volin, The full spectrum of AdS₅/CFT₄ I: Representation theory and one-loop Q-system, *J. Phys. A* **51**, 165401 (2018).
- [53] N. Gromov, F. Levkovich-Maslyuk, and G. Sizov, Quantum spectral curve and the numerical solution of the spectral problem in AdS₅/CFT₄, *J. High Energy Phys.* **06** (2016) 036.
- [54] L. F. Alday and J. Maldacena, Comments on gluon scattering amplitudes via AdS/CFT, *J. High Energy Phys.* **11** (2007) 068.
- [55] C. Meneghelli, *Proceedings of the London Integrability Journal Club* (2020), <https://youtu.be/kst1zikji8>.
- [56] P. S. Howe and P. C. West, AdS/SCFT in superspace, *Classical Quantum Gravity* **18**, 3143 (2001).
- [57] N. Drukker and D. J. Gross, An exact prediction of $N = 4$ SUSYM theory for string theory, *J. Math. Phys. (N.Y.)* **42**, 2896 (2001).
- [58] V. Pestun, Localization of the four-dimensional $N = 4$ SYM to a two-sphere and 1/8 BPS Wilson loops, *J. High Energy Phys.* **12** (2012) 067.
- [59] D. Simmons-Duffin, A semidefinite program solver for the conformal bootstrap, *J. High Energy Phys.* **06** (2015) 174.
- [60] W. Landry and D. Simmons-Duffin, Scaling the semidefinite program solver SDPB, [arXiv:1909.09745](https://arxiv.org/abs/1909.09745).